The optical properties of tropospheric soot aggregates determined with the DDA (Discrete Dipole Approximation) method

Krzysztof Skorupski[a]

[a]Wroclaw University of Technology, Chair of Electronics and Photonics Metrology, Boleslawa Prusa 53/55, 50-317 Wroclaw, Poland

ABSTRACT

Black carbon particles soon after emission interact with organic and inorganic matter. The primary goal of this work was to approximate the accuracy of the DDA method in determining the optical properties of such composites. For the light scattering simulations the ADDA code was selected and the superposition T-Matrix code by Mackowski was used as the reference algorithm. The first part of the study was to compare alternative models of a single primary particle. When only one material is considered the largest averaged relative extinction error is associated with black carbon ($\delta C_{ext} \approx 2.8\%$). However, for inorganic and organic matter it is lowered to $\delta C_{ext} \approx 0.75\%$. There is no significant difference between spheres and ellipsoids with the same volume, and therefore, both of them can be used interchangeably. The next step was to investigate aggregates composed of $N_p = 50$ primary particles. When the coating is omitted, the averaged relative extinction error is $\delta C_{ext} \approx 2.6\%$. Otherwise, it can be lower than $\delta C_{ext} < 0.2\%$.

Keywords: discrete dipole approximation, light scattering, black carbon, soot

1. INTRODUCTION

Black carbon particles are a product of incomplete combustion of carbon-based fuels.[1] Soon after emission they connect to each other and create complex structures, namely aggregates. They can consist even of a few hundreds primary particles (which are usually modeled as spheres positioned in point contact). Additionally, they reveal fractal properties,[2] and therefore, their complex geometry can be approximated by the following equation:[3]

$$N_p = k_f \left(\frac{R_g}{r_p} \right)^{D_f}. \tag{1}$$

The radius of gyration is denoted as R_g. N_p is the number of primary particles with the radius r_p. The fractal dimension D_f defines the compactness of the structure and the last parameter, namely k_f, is the fractal prefactor. The equation is true for monodisperse particles positioned in point contact. However, even if connections between primary particles exist,[4] they intersect[4,5] or are polydisperse,[6] aggregates do not loose their fractal properties.[7] Yet, the value of D_f might be increased.[6] There are many different algorithms for creating fractal-like aggregate models, e.g. DLCA (Diffusion Limited Cluster-Cluster Aggregation)[8] or RLCA (Reaction Limited Cluster-Cluster Aggregation).[9] In this study, the tunable algorithm proposed by Filippov et al. was used.[10,11] It guarantees that Eq. (1) is true for every step of the aggregation process. More information about fractal-like aggregates and their optical properties can be found elsewhere.[6,12]

In this work, the morphological parameters of BC aggregates were: $D_f = 2.2$, $k_f = 0.8$ and $r_p = 15nm$. Selected values were based on different measurements which can be found in the literature, e.g. in the work by Adachi et al.[13] Note, that they are rough approximations and might vary across publications.[14–18] Many different techniques for retrieving morphological parameters are known. Each of them is based on a different algorithm, and therefore, might lead to slightly different results.[19–32] The complex refractive index of black carbon m_c was based on the work by Chang et al.[33] who studied particles generated in propane-oxygen flame (see Fig. 1). The

E-mail: krzysztof.skorupski@pwr.edu.pl

Modeling Aspects in Optical Metrology V, edited by Bernd Bodermann, Karsten Frenner, Richard M. Silver,
Proc. of SPIE Vol. 9526, 95260N · © 2015 SPIE · CCC code: 0277-786X/15/$18 · doi: 10.1117/12.2184634

fuel equivalence ratio was $\phi = 1.8$ and the height above burner was $HAB = 10mm$. Additionally, the selected value of m_c was in agreement with the criterion proposed by Bond et al.[34]

Black carbon is not the only material which can be found in tropospheric soot particles.[35] Furthermore, its volume fraction is relatively low and can be estimated as ca. 7%.[36] Soon after emission black carbon interact with organic and inorganic matter what significantly alter its optical properties. Here, sulphate particles and organic acids are also studied. In contrast to black carbon, their absorption properties are negligible in the visible part of the electromagnetic spectrum. The refractive index for sulphate m_s was based on the OPAC database[37] and the refractive index for organic acids m_a was adapted from the work by Myhre et. al.[38] (see Fig. 1).

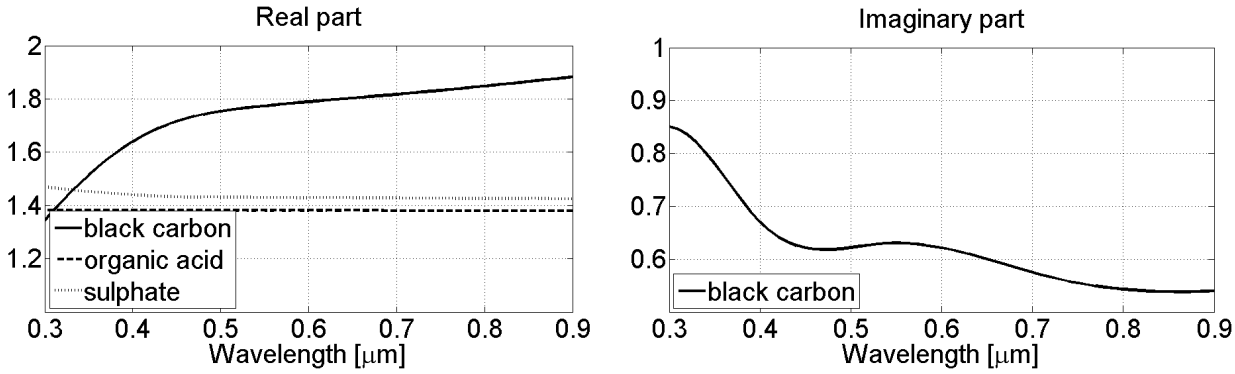

Figure 1: Refractive indices used in this study. The imaginary part of the complex refractive index for sulphate and organic acid is negligible.

Many alternative techniques can be used to model the light scattering phenomenon.[39] Here, for the reference code the superposition T-Matrix algorithm by Mackowski was selected.[40] It gives accurate results providing that the scatterer is composed of non-intersecting spheres. Due to this limitation it could not be used in the final part of the study where more complex structures were investigated. The second technique was DDA (Discrete Dipole Approximation).[41–44] It can predict the amount of the light scattered by any geometry composed of a sufficient number of volume elements (dipoles). However, it can be much more time consuming, especially when the imaginary part of the complex refractive index m is large.[45] For this work the ADDA algorithm, which is widely recognized by the light scattering community, was choosen.[46] Light scattering techniques have been successfully used to characterize many different objects, including e.g. erythrocytes and fibres.[47–52]

The incident wavelength varied from $\lambda = 300nm$ to $\lambda = 900nm$ with the step $\Delta\lambda = 20nm$. ADDA parameters were optimized for black carbon.[53] It was the only absorbing material in the study, and therefore, it had the most significant impact on the light scattering error. The polarizability expression was IGT and the volume correction procedure was not used. The averaged relative extinction error δC_{ext} was the arithmetic mean of all absolute relative errors $|\delta C(\lambda)_{ext}|$. Unless otherwise specified, the results were not averaged.

2. SIMULATION RESULTS

In the preliminary part of the study a single black carbon particle with the radius $r_p = 15nm$ was generated. Next, it was coated with an external layer (organic acid) with a variable thickness t_c, as presented in Fig. 2. The refractive indices of both materials, namely m_c and m_a, were associated with the incident wavelength λ_0. All results (ADDA and T-Matrix) were compared and the averaged extinction error δC_{ext} was calculated, see Tab. 1. It shows that the simulation error does not necessarily diminish along with the number of volume elements (dipoles). This phenomenon might be associated with the fact that the volume correction procedure was not used and the volume of the composite particle was slightly different from the reference one (i.e. the volume of a sphere with the radius $r = r_p + t_c$). Additionally, the DDA mesh must resemble the investigated geometry, what is difficult when the external organic layer is relatively thin. For further study, the value of $d = 2.4nm$ was chosen. It is recommended to put at least $N_{d,x} = 10$ volume elements (dipoles) along the smallest dimension of

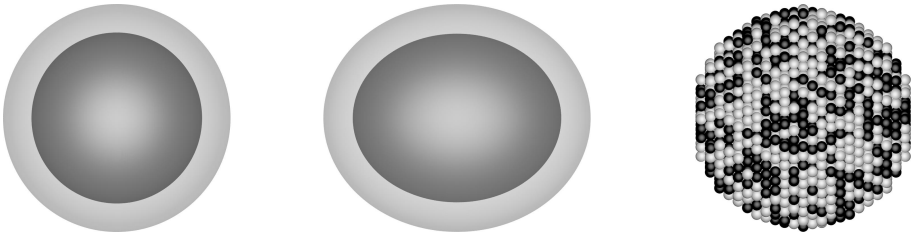

Figure 2: Three geometries used in the first part of the study. They are composed of two materials: black carbon (coloured in black) and organic matter (coloured in gray). Left) A spherical BC particle covered by an external organic layer. Middle) An ellipsoidal BC particle covered by an external organic layer. Right) A spherical particle composed of mixed materials.

Table 1: The averaged extinction error δC_{ext} for a coated, spherical BC particle. The distance between volume elements (dipoles) in the resulting mesh is denoted as d.

d $[nm]$	$t_c = 5nm$	$t_c = 10nm$	$t_c = 15nm$	$t_c = 20nm$
3.00	6.31	8.71	6.14	7.15
2.40	1.77	0.23	0.91	0.86
2.00	2.38	0.68	1.93	0.39
1.50	0.18	1.12	0.87	0.83
1.00	0.47	0.51	0.91	0.89
0.75	0.40	0.54	0.35	0.45
0.60	0.51	0.48	0.46	0.60

the investigated geometry (in this case the internal BC particle). Here, it was $N_{d,x} = 13$ ($N_d = 1021$). Next, three different particles with the radius $r_p = 15nm$ were generated. The averaged relative extinction error was $\delta C_{ext} = 2.71\%$ (black carbon), $\delta C_{ext} = 0.53\%$ (organic acid) and $\delta C_{ext} = 0.67\%$ (sulphate). As expected, the maximum error was observed for the first material. However, its value, which is in agreement with the previous study,[53] was not surprising. The optical properties of the investigated spheres are presented in Fig. 3.

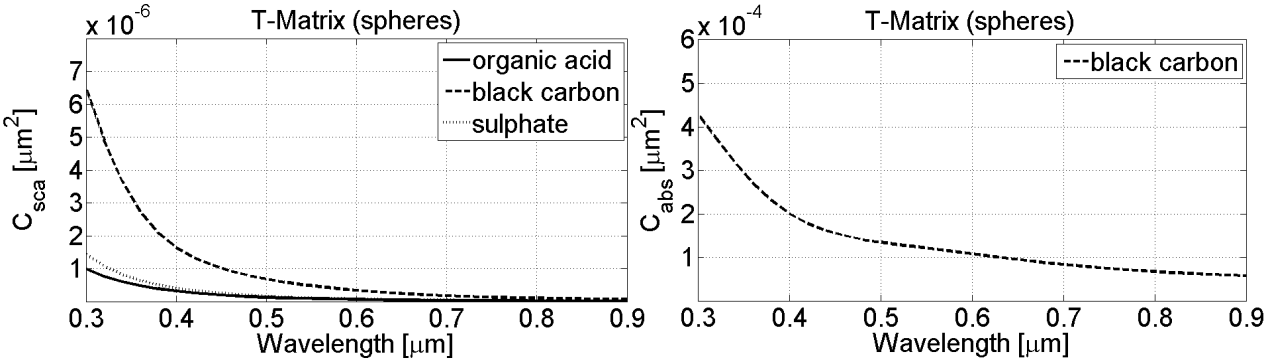

Figure 3: The scattering cross section C_{sca} and the absorption cross section C_{abs} for a single, uncoated particle with the radius $r_p = 15nm$. The superposition T-Matrix algorithm was used.

The light scattering results for a coated black carbon particle are presented in Fig. 4. They show that the scattering cross section C_{sca} is significantly enhanced by the external layer. Additionally, the absorption cross section C_{abs} also increases along with the thickness of the coat t_c. However, these changes are not as significant as for C_{sca}.

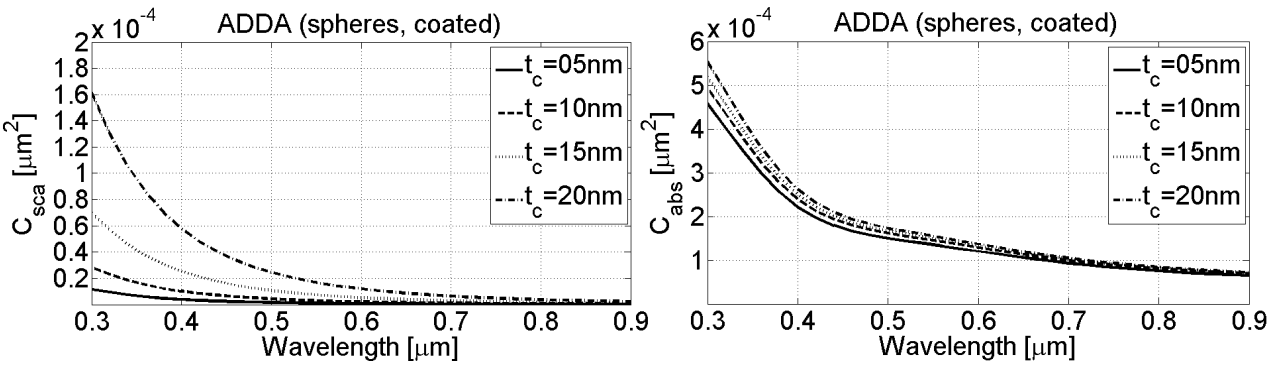

Figure 4: The scattering cross section C_{sca} and the absorption cross section C_{abs} for coated particles. The ADDA algorithm was used.

Next, to investigate the impact of the particle shape on the light scattering results, an ellipsoid was generated (see Fig. 2). Its dimensions were $r_{p,x} \approx 14.26nm$, $r_{p,y} \approx 17.75nm$ and $r_{p,x} \approx 13.33nm$. Therefore, its volume was equal to the volume of the core black carbon particle with the radius $r_p = 15nm$. Because the geometry was not symmetrical the results were orientationally averaged using the Romberg integration technique in the adaptive regime.[54] The estimated integration error was 0.001 and the maximum number of orientations was 256. The distance between volume elements (dipoles) was $d = 2.4nm$ and the results were compared to those calculated with the superposition T-Matrix code for coated, spherical particles. The resulting averaged extinction error was $\delta C_{ext} = 1.89\%$ ($t_c = 5nm$), $\delta C_{ext} = 0.87\%$ ($t_c = 15nm$), $\delta C_{ext} = 0.84\%$ ($t_c = 15nm$) and $\delta C_{ext} = 0.75\%$ ($t_c = 20nm$). The most significant, but still barely visible by the naked eye, difference was observed for $t_c = 5nm$, where the absorption cross section C_{abs} was increased. Nevertheless, ellipsoidal particles (providing that their size ratio is not very distinct) can be modeled as spheres.

The aim of the next part of the study was to check whether the position of volume elements (dipoles) can significantly alter the light scattering results. Four different meshes of coated particles were generated ($d = 2.4nm$). However, this time volume elements (dipoles) were positioned at random, what is presented in Fig. 2. The volume ratio of both materials was not altered. As before, because the investigated geometries were not symmetrical, the results were orientationally averaged. The resulting averaged extinction error was $\delta C_{ext} = 5.87\%$ ($t_c = 5nm$), $\delta C_{ext} = 6.49\%$ ($t_c = 15nm$), $\delta C_{ext} = 11.13\%$ ($t_c = 15nm$) and $\delta C_{ext} = 13.73\%$ ($t_c = 20nm$). The results are presented in Fig. 5. This time changes were more visible, especially for thick layers. The absorption cross section C_{abs} did not increased along with the coat size, what was observed in the previous study.

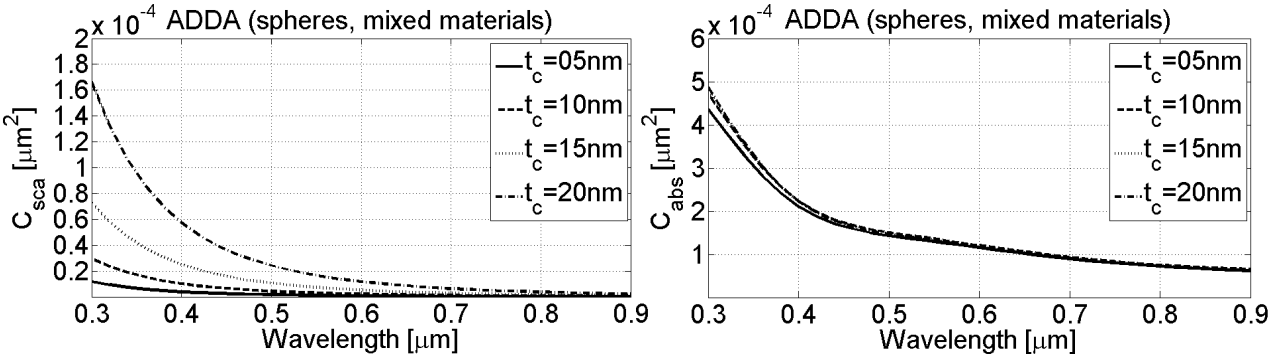

Figure 5: The scattering cross section C_{sca} and the absorption cross section C_{abs} for coated particles. The ADDA algorithm was used and volume elements (dipoles) were positioned at random (see Fig. 2).

For the following part of the study two fractal-like aggregate models were generated, as presented in Fig. 6. They consisted of $N_p = 50$ primary particles with the radius $r_p = 15nm$. The first of them was composed of $N_{p,c} = 25$ particles of black carbon and $N_{p,s} = 25$ sulphate particles. The composition of the second one was $N_{p,c} = 19$, $N_{p,s} = 16$ and $N_{p,a} = 15$ (organic acid). No connections were implemented and the distance between volume elements (dipoles) was $d = 2.4nm$. To precisely compare both scattering algorithms and exclude possible errors caused by the averaging procedure, only fixed positions were investigated. Therefore, in Fig. 7 two orthogonal polarization states are presented, namely pol. A (plane ZX) and pol. B (plane ZY). The averaged extinction errors for the geometry without organic acid were $\delta C_{ext} \approx 2.25\%$ (pol. A) and $\delta C_{ext} \approx 2.43\%$ (pol. B). For the second geometry they were estimated as $\delta C_{ext} \approx 2.61\%$ (pol. A) and $\delta C_{ext} \approx 2.47\%$ (pol. B) respectively. These values are with agreement with the previous study.

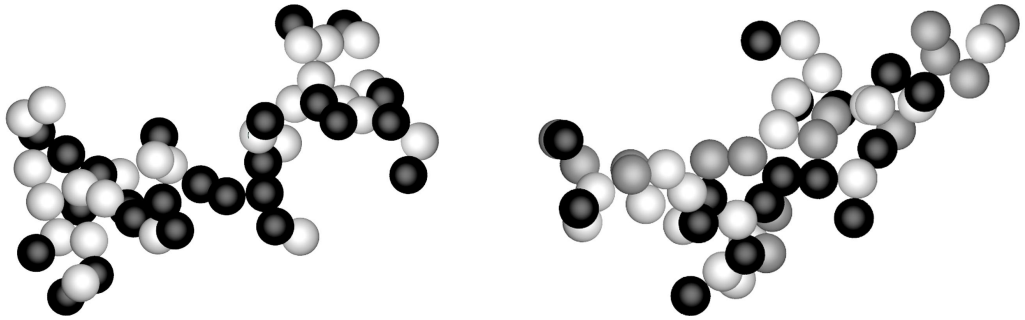

Figure 6: Two fractal-like aggregates composed of $N_p = 50$ primary particles with the radius $r_p = 15nm$. The components are: black carbon (black spheres), sulphate (white spheres) and organic acid (gray spheres).

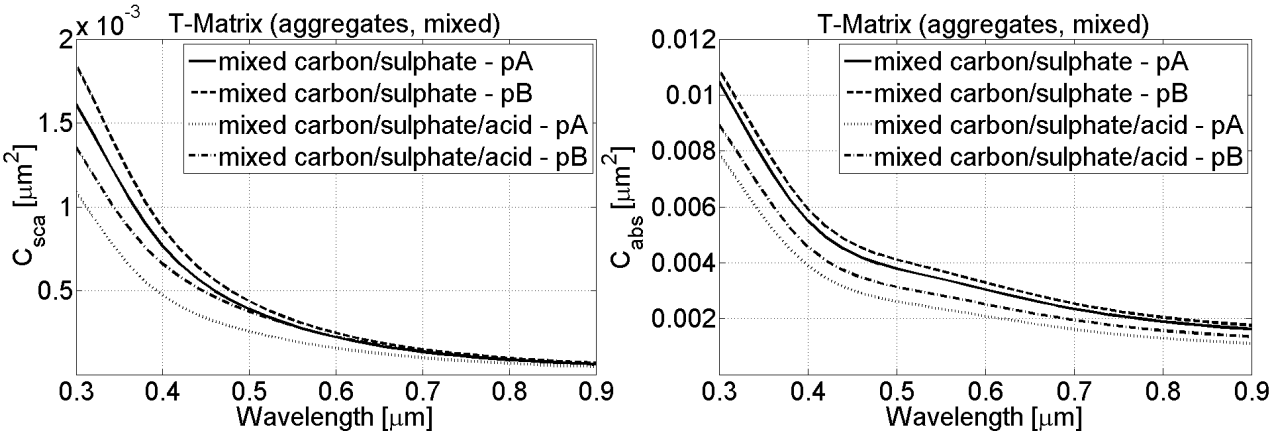

Figure 7: The scattering cross section C_{sca} and the absorption cross section C_{abs} for fractal-like aggregates composed of mixed particles (see Fig. 6). The superposition T-Matrix algorithm was used.

Next, two coated fractal-like aggregates, which are presented in Fig. 8, were generated. One of them was made of $N_{p,c} = 50$ primary particles with the radius $r_p = 15nm$. The composition of the second one was $N_{p,c} = 25$ (black carbon) and $N_{p,s} = 25$ (sulphate). In both cases the thickness of the organic layer was $t_c = 5nm$ and particles were positioned in point contact. The simulation parameters and the distance between volume elements (dipoles), i.e. $d = 2.4nm$, were identical to those used in the previous study. In this case the averaged extinction error was not greater than $\delta C_{ext} < 0.2\%$ in every case, regardless of the number of materials or the polarization

state. This value was much lower than expected (see Tab. 1). The light scattering results are presented in Fig. 9.

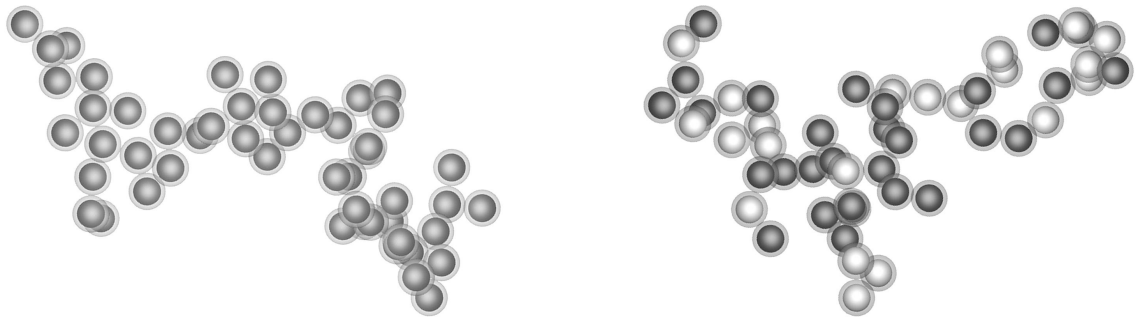

Figure 8: Two fractal-like aggregates composed of coated particles with the radius $r_p = 20nm$ (including the external layer, i.e. $t_c = 5nm$). Left) Coated black carbon $N_{p,c} = 50$ particles. Right) Coated black carbon $N_{p,c} = 25$ and sulphate $N_{p,s} = 25$ particles.

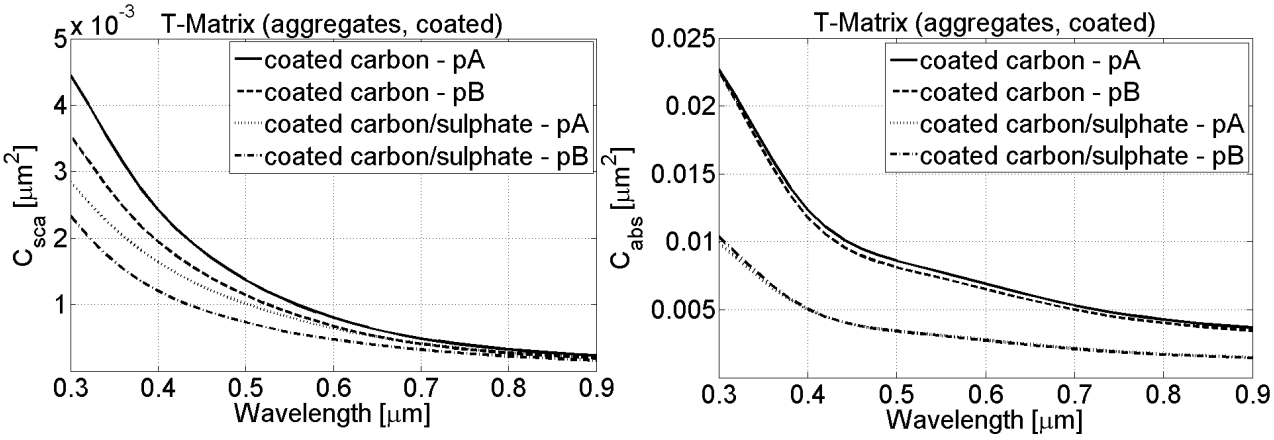

Figure 9: The scattering cross section C_{sca} and the absorption cross section C_{abs} for fractal-like aggregates composed of coated particles (see Fig. 8). The superposition T-Matrix algorithm was used.

Finally, a more realistic soot model was created. The core element was a fractal-like aggregate composed of $N_{p,c} = 50$ primary particles. They were modeled as ellipsoids generated at random with the following parameters: $r_{p,c,i} = 15nm$ and $\sigma_{c,i} = 1.5nm$ where $\sigma_{c,i}$ is the standard deviation and i is the axis (X, Y or Z). The volume of the structure was equivalent to the volume of an assembly of $N_p = 50$ spherical particles with the radius $r_p = 15nm$. Next, connection between particles were implemented. They were modeled as cylinders with the size parameter $Y_{con} = 0.5$, i.e. the radius of each cylinder was half the radius of the smaller of two spheres inscribed in connected ellipsoidal particles. More information about modelling of the necking phenomenon can be found elsewhere.[4] Later, five $N_{p,s}$ ellipsoidal sulphate particles were added. They were generated at random with the following parameters: $r_{p,s,i} = 30nm$ and $\sigma_{s,i} = 3nm$. The volume of each particle was equivalent to the volume of a spherical particle with the radius $r_p = 30nm$. Every sulphate particle was positioned in point contact with at least one black carbon particle. Moreover, the number of surrounding (not necessarily touching) particles was at its maximum. Finally, every neck and every primary particle was coated with an external organic layer with a variable thickness t_c. The generated soot particle is presented in Fig. 10 and the resulting diagrams can be found in Fig. 11 and in Fig. 12. Similarly to the study for a single coated particle the scattering C_{sca}

and the absorption C_{abs} cross sections increase along with the coat thickness t_c. In this case, due to the complex shape of the investigated geometry, only the DDA algorithm was used.

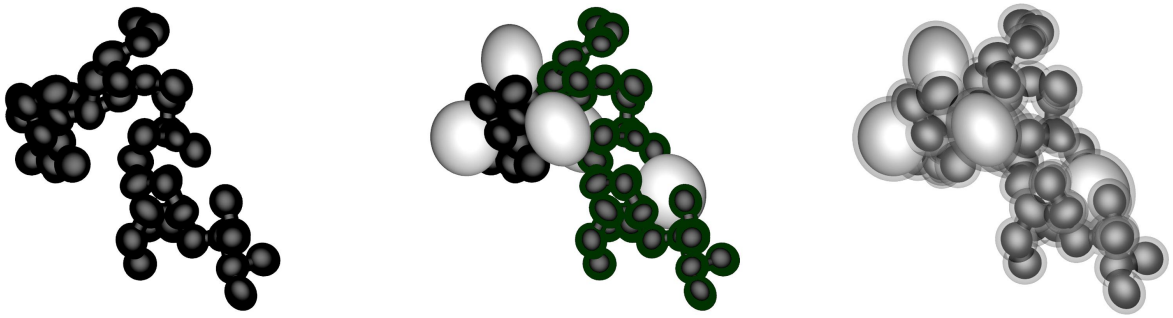

Figure 10: The soot particle used in the study. The core black carbon fractal aggregate (coloured in black) is composed of $N_{p,c}$ connected ellipsoidal particles. The sulphate particles are coloured in white. The thickness of the coat is $t_c = 5nm$.

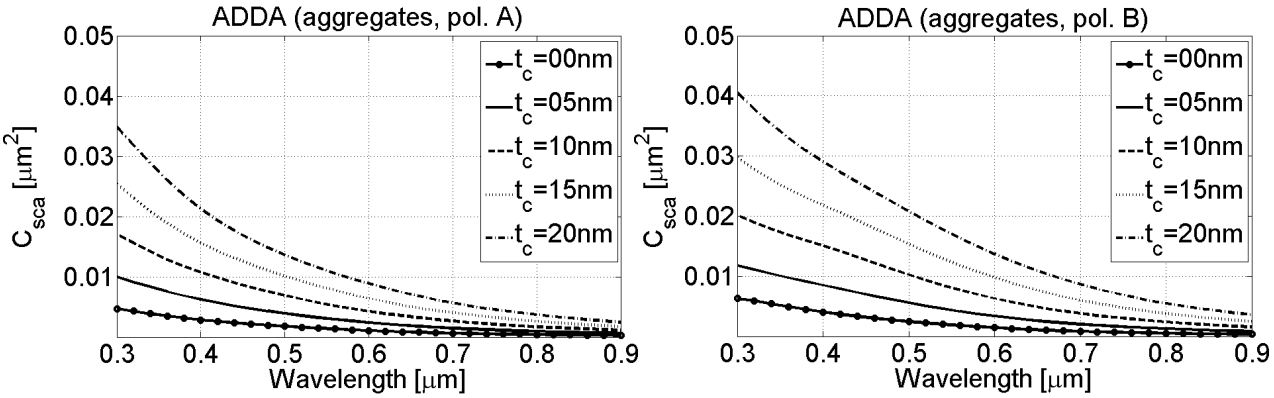

Figure 11: The scattering cross section C_{sca} for the soot particle used in the study. The DDA algorithm was used.

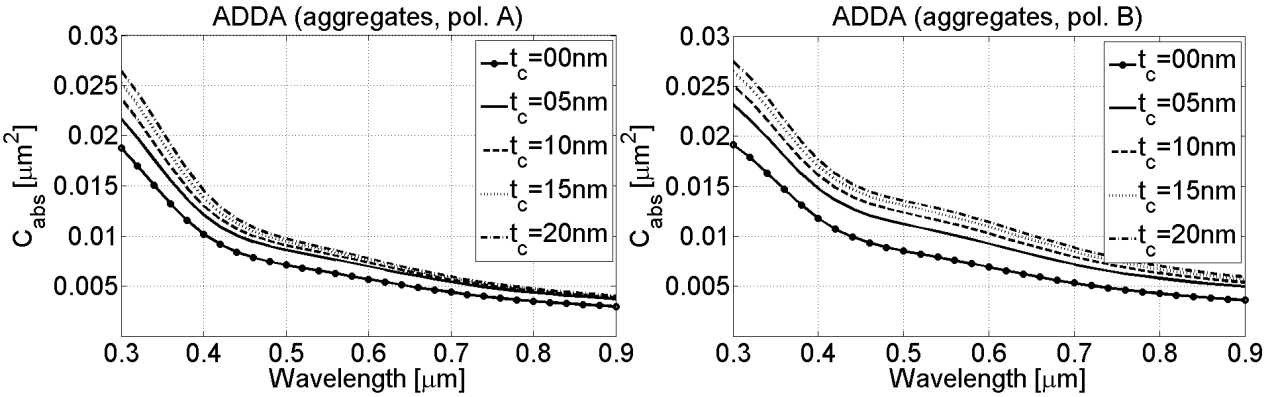

Figure 12: The absorption cross section C_{abs} for the soot particle used in the study. The DDA algorithm was used.

3. CONCLUSIONS

The main goal of this work was to generate realistic soot aggregate models and approximate the accuracy of DDA simulations.[55] As the reference program the superposition T-Matrix code by Mackowski was used. Three different materials were investigated, namely: black carbon, organic acid and sulphate. The most significant simulation error was associated with the most absorbing material, i.e. black carbon. No large difference between coated spherical and ellipsoidal particles was observed, and therefore, they can be used interchangeably. The position of volume elements (dipoles) in the resulting DDA mesh is crucial. They must precisely resemble the original geometry. Otherwise, the increase in absorption caused by an external layer might be diminished. When large fractal-like aggregates composed of mixed, uncoated particles are investigated, the averaged extinction error δC_{ext} is similar to the one obtained for a single black carbon particle (the most absorbing material). However, when a fractal-like aggregate is made up of coated particles, δC_{ext} is much smaller and there is almost no difference between the two investigated scattering algorithms, i.e. ADDA and T-Matrix. Finally, when more realistic geometries are examined, the scattering C_{sca} and the absorption C_{abs} cross section increase along with the coat thickness t_c.

REFERENCES

[1] Bond, T., "Spectral dependence of visible light absorption by carbonaceous particles emitted from coal combustion," *Geophysical Research Letters* **28**, 4075–4078 (2001).

[2] Mandelbrot, B., [*The Fractal Geometry of Nature*], W. H. Freeman and Co. (1982).

[3] Sorensen, C. M., "Light scattering by fractal aggregates: A review," *Aerosol Science and Technology* **35**, 648–687 (2001).

[4] Skorupski, K. and Mroczka, J., "Effect of the necking phenomenon on the optical properties of soot particles," *Journal of Quantitative Spectroscopy and Radiative Transfer* **141**, 40–48 (2014).

[5] Brasil, A. M., Farias, T. L., Carvalho, G., and Koylu, U. O., "Numerical characterization of the morphology of aggregated particles," *Journal of Aerosol Science* **32**, 489–508 (2001).

[6] Meakin, P., "A historical introduction to computer models for fractal aggregates," *Journal of Sol-Gel Science and Technology* **15**, 97–117 (1999).

[7] Oh, C. and Sorensen, C. M., "The effect of overlap between monomers on the determination of fractal cluster morphology," *Journal of Colloid and Interface Science* **193**, 17–25 (1997).

[8] Meakin, P., "Formation of fractal clusters and networks by irreversible diffusion-limited aggregation," *Physical Review Letters* **51**, 1119–1122 (1983).

[9] Jullien, R. and Botet, R., "Hierarchical model for chemically limited cluster-cluster aggregates," *Journal of Physics A: Mathematical and General* **17**, L639L643 (1984).

[10] Filippov, A., Zurita, M., and Rosner, D., "Fractal-like aggregates: Relation between morphology and physical properties," *Journal of Colloid and Interface Science* **229**, 261–273 (2000).

[11] Skorupski, K., Mroczka, J., Wriedt, T., and Riefler, N., "A fast and accurate implementation of tunable algorithms used for generation of fractal-like aggregate models," *Physica A: Statistical Mechanics and its Applications* **404**, 106–117 (2014).

[12] Skorupski, K., Mroczka, J., Riefler, N., Oltmann, H., Will, S., and Wriedt, T., "Impact of morphological parameters onto simulated light scattering patterns," *Journal of Quantitative Spectroscopy and Radiative Transfer* **119**, 53–66 (2013).

[13] Adachi, K., Chung, S., Friedrich, H., and Buseck, P. R., "Fractal parameters of individual soot particles determined using electron tomography: implications for optical properties," *Journal of geophysical research* **112**, D14202 (2007).

[14] Sorensen, C. M. and Feke, G. D., "The morphology of macroscopic soot," *Aerosol Science and Technology* **25**, 328–337 (1996).

[15] Poppel, L. L., Friedrich, H., Spinsby, J., Chung, S. H., Seinfeld, J. H., and Buseck, P. R., "Electron tomography of nanoparticle clusters: Implications for atmospheric lifetimes and radiative forcing of soot," *Geophysical Research Letters* **32**, L24811,doi:10.1029/2005GL024461 (2005).

[16] Kittelson, D., "Engines and nanoparticles: A review," *Journal of Aerosol Science* **29**, 575–588 (1998).

[17] Maricq, M., "Chemical characterization of particulate emissions from diesel engines: A review," *Journal of Aerosol Science* **38**, 1079–1118 (2007).
[18] Burtscher, H., "Physical characterization of particulate emissions from diesel engines: A review," *Journal of Aerosol Science* **36**, 896–932 (2005).
[19] Mroczka, J. and Szczuczynski, D., "Inverse problems formulated in terms of first-kind fredholm integral equations in indirect measurements," *Metrology and Measurement Systems* **16**, 333–357 (2009).
[20] Mroczka, J. and Szczuczynski, D., "Improved regularized solution of the inverse problem in turbidimetric measurements," *Applied Optics* **5**, 4591 (2010).
[21] Mroczka, J. and Szczuczynski, D. K., "Simulation research on improved regularized solution of the inverse problem in spectral extinction measurements," *Applied Optics* **51**, 1715–1723 (2012).
[22] Mroczka, J. and Szczuczynski, D., "Improved technique of retrieving particle size distribution from angular scattering measurements," *Journal of Quantitative Spectroscopy and Radiative Transfer* **129**, 48–59 (2013).
[23] Mroczka, J., Wozniak, M., and Onofri, F. R. A., "Algorithms and methods for analysis of the optical structure factor of fractal aggregates," *Metrology and Measurements Systems* **19**, 459–470 (2012).
[24] Will, S., Schraml, S., Bader, K., and A.Leipertz, "Performance characteristics of soot primary particle size measurements by time-resolved laser-induced incandescence," *Applied Optics* **37**, 5647–5658 (1998).
[25] Iuliis, S. D., Cignoli, F., and Zizak, G., "Two-color laser-induced incandescence (2C-LII) technique for absolute soot volume fraction measurements in flames," *Applied Optics* **44**, 7–8 (2005).
[26] Ryser, R., Gerber, T., and Dreier, T., "Soot particle sizing during high-pressure diesel spray combustion via time-resolved laser-induced incandescence," *Combustion and Flame* **156**, 120–129 (2009).
[27] Oltmann, H., Reimann, J., and Will, S., "Single-shot measurement of soot aggregate sizes by wide-angle light scattering (WALS)," *Applied Physics B: Lasers and Optics* **106**, 171–183 (2012).
[28] Oltmann, H., Reimann, J., and Will, S., "Wide-angle light scattering (WALS) for soot aggregates characterization," *Combustion and Flame* **157**, 516–522 (2010).
[29] Wozniak, M., Onofri, F. R. A., Barbosa, S., Yon, J., and Mroczka, J., "Comparison of methods to derive morphological parameters of multi-fractal samples of particle aggregates from tem images," *Journal of Aerosol Science* **47**, 12–26 (2012).
[30] Brasil, A. M., Farias, T. L., and Carvalho, G., "A recipe for image characterization of fractal-like aggregates," *Journal of Aerosol Science* **30**, 1379–1389 (1999).
[31] Czerwinski, M., Mroczka, J., Girasole, T., Gouesbet, G., and Grehan, G., "Light-transmittance predictions under multiple-light-scattering conditions. I. direct problem: hybrid-method approximation," *Applied Optics* **40**, 1514–1524 (2001).
[32] Czerwinski, M., Mroczka, J., Girasole, T., Gouesbet, G., and Grehan, G., "Light-transmittance predictions under multiple-light-scattering conditions. II. inverse problem: particle size determination," *Applied Optics* **40**, 1525–1531 (2001).
[33] Chang, H. and Charalampopoulos, T., "Determination of the wavelength dependence of refractive indices of flame soot," *Proceedings: Mathematical and Physical Sciences* **430**, 577–591 (1990).
[34] Bond, T. and Bergstrom, R., "Light absorption by carbonaceous particles: an investigative review," *Aerosol Science and Technology* **40**, 27–67 (2006).
[35] Heintzenberg, J., "Fine particles in the global troposphere: A review," *Tellus* **41B**, 149–160 (1989).
[36] Adachi, K., Chung, S., and Buseck, P., "Shapes of soot aerosol particles and implications for their effects on climate," *Journal of geophysical research* **115**, D15206 (2010).
[37] Hess, M., Koepke, P., and Schult, I., "Optical properties of aerosols and clouds: The software package opac," *Bulletin of the American Meteorological Society* **79**, 831–844 (1998).
[38] Myhre, C. and Nielsen, C., "Optical properties in the UV and visible spectral region of organic acids relevant to tropospheric aerosols," *Atmospheric Chemistry and Physics* **4**, 1759–1769 (2004).
[39] Wriedt, T., "Light scattering theories and computer codes," *Journal of Quantitative Spectroscopy and Radiative Transfer* **110**, 833–8433 (2009).
[40] Mackowski, D. and Mischenko, M., "A multiple sphere t-matrix fortran code for use on parallel computer clusters," *Journal of Quantitative Spectroscopy and Radiative Transfer* **112**, 2182–2192 (2011).

[41] Purcell, E. M. and Pennypacker, C. R., "Scattering and absorption of light by nonspherical dielectric grains," *The Astrophysical Journal* **186**, 707–714 (1973).

[42] Draine, B. T. and Flatau, P. J., "Discrete dipole approximation for scattering calculations," *Journal of the Optical Society of America A* **11**, 1491–1499 (1994).

[43] Penttila, A., Zubko, E., Lumme, K., Muinonen, K., Yurkin, M., Draine, B., Rahola, J., Hoekstra, A., and Shkuratov, Y., "Comparison between discrete dipole implementations and exact techniques," *Journal of Quantitative Spectroscopy and Radiative Transfer* **106**, 417–436 (2007).

[44] Yurkin, M. and Hoekstra, A., "The discrete dipole approximation: An overview and recent developments," *Journal of Quantitative Spectroscopy and Radiative Transfer* **106**, 558–589 (2007).

[45] Yurkin, M., Min, M., and Hoekstra, A., "Application of the discrete dipole approximation to very large refractive indices: Filtered coupled dipoles revived," *Physical Review E* **82**, http://dx.doi.org/10.1103/PhysRevE.82.036703 (2010).

[46] Yurkin, M. and Hoekstra, A., "The discrete-dipole-approximation code adda: Capabilities and known limitations," *Journal of Quantitative Spectroscopy and Radiative Transfer* **112**, 2234–2247 (2011).

[47] Wriedt, T., Hellmers, J., Eremina, E., and Schuh, R., "Light scattering by single erythrocyte: Comparison of different methods," *Journal of Quantitative Spectroscopy and Radiative Transfer* **100**, 444–456 (2006).

[48] Nilsson, A., Alsholm, P., Karlsson, A., and Andersson-Engels, S., "T-matrix computations of light scattering by red blood cells," *Applied Optics* **37**, 2735–2748 (1998).

[49] Mroczka, J. and Wysoczanski, D., "Plane-wave and gaussian-beam scattering on an infinite cylinder," *Optical Engineering* **39**, 736–770 (2000).

[50] Girasole, T., Gouesbet, G., Grehan, G., Toulouzan, J. L., Mroczka, J., Ren, K., and Wysoczanski, D., "Cylindrical fibre orientation analysis by light scattering. part II: Experimental aspects," *Particle and Particle Systems Characterization* **14**, 211218 (1997).

[51] Girasole, T., Bultynck, H., Gouesbet, G., Grehan, G., Meur, F. L., Toulouzan, J. L., Mroczka, J., and Wysoczanski, D., "Cylindrical fibre orientation analysis by light scattering. part I: Numerical aspects," *Particle and Particle Systems Characterization* **14**, 163–174 (1997).

[52] Girasole, T., Toulouzan, J. L., Mroczka, J., and Wysoczanski, D., "Fiber orientation and concentration analysis by light scattering: Experimental setup and diagnosis," *Review of Scientific Instruments* **68**, 2805–2811 (1997).

[53] Skorupski, K., "Using the DDA (discrete dipole approximation) method in determining the extinction cross section of black carbon," *Metrology and Measurement Systems* **22**, 153–164 (2015).

[54] Riefler, N., Stasio, S., and Wriedt, T., "Structural analysis of clusters using configurational and orientational averaging in light scattering analysis," *Journal of Quantitative Spectroscopy and Radiative Transfer* **89**, 323–342 (2004).

[55] Mroczka, J., "The cognitive process in metrology," *Measurement* **46**, 2896–2907 (2013).